INTERNATIONAL JOURNAL OF PRECISION ENGINEERING AND MANUFACTURING Vol. 17, No. 9, pp. 1113-1119 SEPTEMBER 2016 / 1113
DOI: 10.1007/s12541-016-0135-4 ISSN 2234-7593 (Print) / ISSN 2005-4602 (Online)

Accurate Calibration of Systematic Errors for Car-Like Mobile Robots using Experimental Orientation Errors

Daun Jung[1], Jihoon Seong[1], Chang-bae Moon[2], Jiyong Jin[1], and Woojin Chung[1,#]

1 Department of Mechanical Engineering, Korea University, 145, Anam-ro, Seongbuk-gu, Seoul, 02841, South Korea
2 School of Mechanical Engineering, Chonnam National University, 77, Yongbong-ro, Buk-gu, Gwangju, 61186, South Korea
Corresponding Author / E-mail: smartrobot@korea.ac.kr, TEL: +82-2-3290-3375, FAX: +82-2-3290-3375

KEYWORDS: Mobile robot, Calibration, Odometry, Localization

One of the essential technologies for autonomous navigation is localization. Localization is important because accurate pose estimation is required for path planning and motion control. In order to improve localization accuracy, a relative positioning method on the basis of accurate odometry is necessary. Odometry calibration methods for two wheel differential drive robots have been researched for many years. However, it is difficult to find odometry calibration methods for car-like mobile robots. In this paper, an accurate calibration method for car-like mobile robots is proposed. Experimentally measured orientation errors were used to improve the accuracy of the calibration method. There are two contributions in this paper. The first is the significant reduction of calibration errors by the use of accurate calibration equation. In the previous research, calibration equation required approximations. However, there is no approximation error in the proposed equation owing to the use of orientation errors, not positional errors. The second is the experimental convenience. The orientations can be easily measured by onboard inertial sensors. Therefore, calibration experiments can be easily carried out in both indoor and outdoor environments. The presented experimental results show that resultant performance of the proposed scheme is superior to the results of the previous research.

Manuscript received: May 22, 2015 / Revised: March 14, 2016 / Accepted: May 12, 2016

1. Introduction

Recently, various studies on autonomous navigation have been carried out.[1,2] Localization is important because accurate pose estimation is required for path planning and motion control.

Odometry using incremental wheel encoder sensors is a fundamental technique for pose estimation of wheeled mobile robots. Odometry implies the computation of the relative pose of a robot from the known initial pose from accumulated encoder data. However, odometry has a well-known drawback that kinematic modeling errors accumulate as the robot's travel distance increases. Calibration is necessary to reduce the odometry errors that occur with increasing travel distance. Improved odometry can significantly reduce the operational costs associated with the installation and maintenance of sensors and landmarks. Improved odometry also reduces the uncertainty of the estimated pose when external sensors cannot be used because of weather or environmental conditions. Use of the Extended Kalman Filter is based on the assumption that the mean of the added Gaussian noise in state transition is zero.[3] For this reason, the EKF-based localization technique is useful when the odometry has a zero mean and white Gaussian noise.

Odometry error sources can be classified as either systematic or nonsystematic errors.[3-6] Systematic errors are specific to vehicles and do not usually change abruptly during navigation. Therefore, systematic errors can be reduced by calibrating the kinematic parameters. Examples of systematic error sources include unequal wheel diameters and errors in the distance between the left and right wheels. Non-systematic errors are caused by interactions between the robot and road conditions, which are stochastic. Examples of nonsystematic error sources include uneven floors, unexpected objects on the floor, and wheel slippages. External sensors can be added to model the uncertainty of nonsystematic errors using the absolute position of the robot as determined from external sensors.[7,8]

Studies related to odometry calibration have been conducted for many years. The UMBmark method[5] is a useful calibration scheme for two wheel differential drive robots. The wheel diameter error and the wheelbase error are calibrated by measuring the final position errors after the test run. During the test run, the robot is driven along a 4m-square path in both the clockwise (CW) and counterclockwise (CCW)

directions. The UMBmark method[5] adopts the assumption that the wheel diameter error and the wheelbase error are independent. In practice, this assumption is invalid because the wheel diameter error and the wheelbase errors simultaneously take place. In addition, approximation by small-angle assumption was adopted in the calibration equations in order to simplify the calibration equations. Small-angle assumption implies $\sin\varphi = \varphi$ and $\cos\varphi = 1$.

Lee[9] proposed an odometry calibration scheme for a two wheel differential drive robot that considers the coupled effect of unequal wheel diameters and wheelbase error. The conventional UMBmark method[5] assumes that the wheel diameter error and wheelbase error are independent. Considering the coupled effect of two error sources improves the odometry calibration accuracy.

Jung[10,11] proposed an odometry calibration scheme for a two wheel differential drive robot that involves measuring the final orientation errors after a test run. Using these orientation error measurements, approximation errors are eliminated, and the calibration accuracy is improved. The conventional UMBmark method[5] involves approximation errors associated with the small-angle approximations used.

It is difficult to find odometry calibration schemes for car-like mobile robots. McKerrow[12] proposed a calibration scheme for steering angle and kinematic parameters of car-like mobile robots. In this scheme, the odometry error is modeled by introducing three parameters to characterize the steering angle and the wheel diameters. Each parameter of McKerrow's odometry model is defined using left and right wheel encoder information. For McKerrow's method,[12] additional range sensor information and range sensor calibration are required.

Lee[13,14] proposed an odometry calibration scheme for a car-like mobile robot that involves measuring the final position errors after a test run. The test track is similar in shape to a 400-m running track. Lee[14] verified that the localization accuracy of the scheme is improved by using the EKF to combine the encoder data from the front wheels and rear wheels.

It has been verified that the odometry calibration accuracy can be improved by using the final orientation errors instead of the final position errors.[10,11] Lee's method for a car-like mobile robot[13,14] is a useful method for calibration of car-like mobile robots. However, Lee's method[13,14] also involves approximation errors associated with small-angle approximations, because Lee's method uses the final position errors and approximation is needed to simplify the calibration equations. In this paper, an accurate calibration scheme for car-like mobile robots that uses experimentally measured orientation errors is proposed. As with the methods for two wheel differential drive robots, the odometry calibration accuracy for car-like mobile robots can be improved using orientation errors rather than position errors.

The remaining parts of this paper are organized as follows. In section 2, the proposed calibration scheme that uses experimentally measured orientation errors is discussed. In section 3, experimental results are presented. Finally, the contributions of this paper are summarized in section 4.

2. Accurate Calibration using Orientation Errors.

In order to calculate the orientation errors caused by each error source, it is assumed that the robot is affected by either wheel diameter error or tread error. The kinematic parameters for each error source are defined as follows.

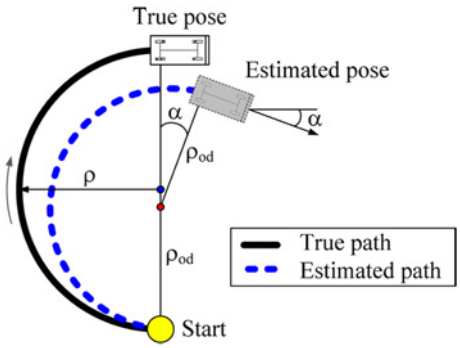

Fig. 1 Orientation error caused by tread error when the robot is driven along a circular path

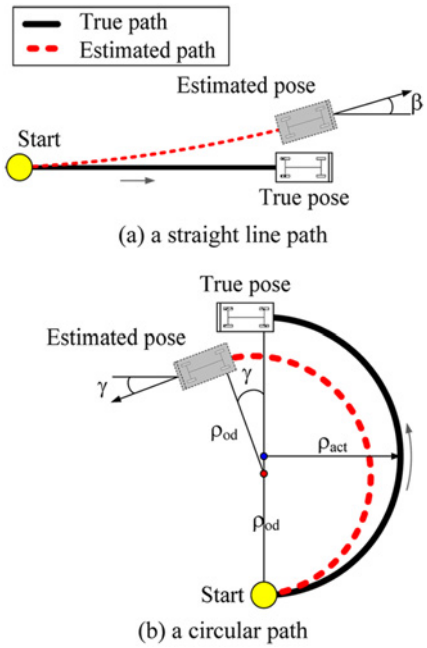

Fig. 2 Orientation errors caused by unequal wheel diameters when the robot is driven along (a) a straight-line path and (b) a circular path

$$E_b = \frac{b_{actual}}{b_{nominal}}$$
$$E_d = \frac{D_R}{D_L} \quad (1)$$

b_{actual} is the actual tread, $b_{nominal}$ is the nominal tread, D_R is the right wheel diameter, and D_L is the left wheel diameter.

Fig. 1 represents orientation error caused by tread error. When the robot has only tread error, orientation error appears after a run along a circular path. The robot moves along a circular path with radius ρ, because the heading direction of a car-like mobile robot depends on the steering direction. However, the estimated path by odometry is a circular path with radius ρ_{od}. From the equation for the arc length, l =

$r \cdot \theta$, orientation error α is caused by the difference in the radii of the circular paths.

Fig. 2 shows orientation errors caused by unequal wheel diameters. When the robot has only wheel diameter errors, orientation error appears after a run along either a straight-line path or a circular path. Orientation error β on the straight-line path and orientation error γ on the circular arc path are caused by the difference in the angular velocities of the left and right wheels. Lee's work[13] shows that orientation error γ can be represented as a function of orientation error β.

$$\gamma = \frac{\pi}{2}\beta \tag{2}$$

Fig. 3 shows orientation errors caused by tread error when the robot is driven along the test track. Orientation error α occurs along the circular path of the test track, as shown in Fig. 1. After test runs in the CW and CCW directions, the final orientation errors caused by tread error are calculated as follows.

Orientation errors caused by tread error when the robot is driven in the CW direction:

$$\begin{aligned}
\theta_0 &= \pi \\
\theta_1 &= \theta_0 = \pi \\
\theta_2 &= \theta_1 - \pi - \alpha = -\alpha \\
\theta_3 &= \theta_2 = -\alpha \\
\theta_4 &= \theta_3 - \pi - \alpha = \pi - 2\alpha \\
\theta_4 - \theta_0 &= -2\alpha
\end{aligned} \tag{3}$$

Orientation errors caused by tread error when the robot is driven in the CCW direction:

$$\begin{aligned}
\theta_0 &= 0 \\
\theta_1 &= \theta_0 = 0 \\
\theta_2 &= \theta_1 + \pi + \alpha = \pi + \alpha \\
\theta_3 &= \theta_2 = \pi + \alpha \\
\theta_4 &= \theta_1 + \pi + \alpha = 2\alpha \\
\theta_4 - \theta_0 &= 2\alpha
\end{aligned} \tag{4}$$

Fig. 4 shows orientation errors caused by unequal wheel diameters when the robot is driven along the test track. Orientation errors β and γ occur as shown in Fig. 2. After the test run in the CW and CCW directions, the final orientation errors caused by unequal wheel diameters are calculated as follows.

Orientation errors caused by wheel diameter error when the robot is driven in the CW direction:

$$\theta_4 - \theta_0 = 2\beta + 2\gamma \tag{5}$$

Orientation errors caused by wheel diameter error when the robot is driven in the CCW direction:

$$\theta_4 - \theta_0 = 2\beta + 2\gamma \tag{6}$$

From Eqs. (2)~(6), the total orientation errors caused by tread error and wheel diameter error in the CW and CCW directions are calculated as follows.

$$\begin{aligned}
\theta_{CW} &= -2\alpha + 2\beta + 2\gamma = -2\alpha + (2+\pi)\beta \\
\theta_{CCW} &= 2\alpha + 2\beta + 2\gamma = 2\alpha + (2+\pi)\beta
\end{aligned} \tag{7}$$

From Eq. (7), orientation errors α and β can be calculated as

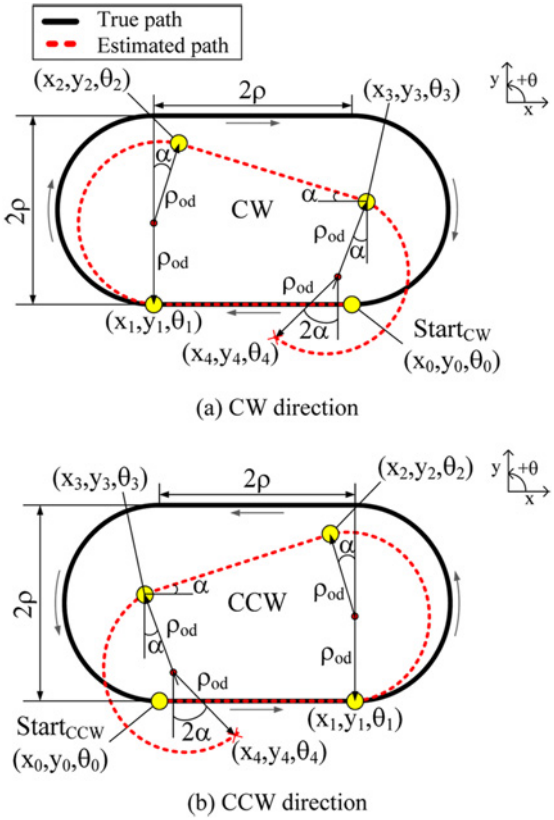

Fig. 3 Orientation errors caused by tread error during the test run

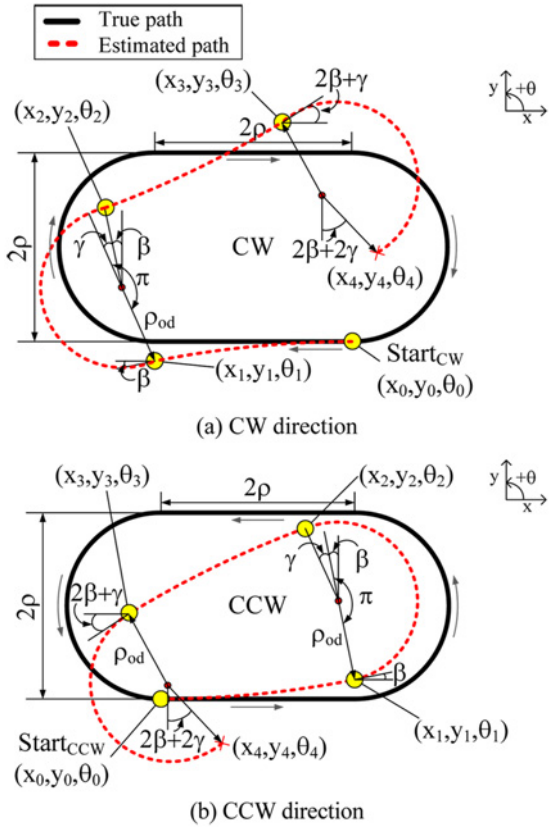

Fig. 4 Orientation errors caused by unequal wheel diameter during the test run

Fig. 5 Experimental environment

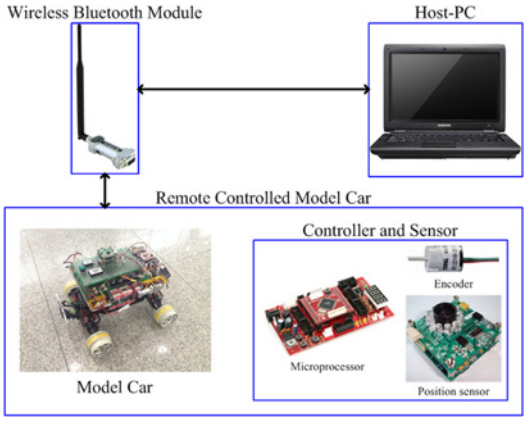

Fig. 6 Configuration of experimental robot system

follows.

$$\alpha = \frac{\theta_{CW} - \theta_{CCW}}{-4}$$
$$\beta = \frac{\theta_{CW} + \theta_{CCW}}{2(2+\pi)} \tag{8}$$

The kinematic parameters defined in Eq. (1) can be estimated using Eq. (8).

$$E_b = \frac{b_{actual}}{b_{nominal}} = \frac{\pi + \alpha}{\pi}$$
$$E_d = \frac{D_R}{D_L} = \frac{R - \frac{b}{2}}{R + \frac{b}{2}}, \quad R = \frac{\rho}{\sin(\beta/2)} \tag{9}$$

In the work of Lee[9] and Jung,[10,11] the coupled effects on spot-turning motion are also calculated. In the method proposed in this paper, this additional term is not calculated because both orientation error α caused by tread error and orientation error γ caused by wheel diameter error are considered.

Compared with Lee's method[13,14] and the proposed method, the proposed method does not need to adopt approximation by small-angle assumption. In the proposed method, calibration equations are derived relatively easily without approximation by using the final orientation errors. Odometry calibration accuracy also can be improved because the errors by approximation are eliminated.

3. Experimental Results

In order to verify the calibration performance of the proposed method, experiments were carried out in a real-world environment. As Fig. 5 shows, the experimental environment was a relatively smooth and flat indoor floor.

Fig. 6 shows configuration of experimental robot system. Experimental robot system consists of a host-PC, a remote controlled model car and wireless Bluetooth module. The host-PC sends control signals to the remote controlled model car and records the experimental data. The remote controlled model car executes the motions according to the control signals from the host-PC. The remote controlled model car includes the microprocessor ATmega128[15,16] for motion control, the rotary encoder RE12D[17] for localization, and the commercial absolute positioning sensor Stargazer[18] for the measurement of the vehicle pose. The Stargazer is a commercially available localization sensor that uses artificial landmarks. The Stargazer system measures the absolute position of the robot in static state with the repeatability of ±1 mm and ±0.5°. The host-PC and the remote controlled model car communicate via the wireless Bluetooth module FB100AS.[19] The following are details of the remote controlled model car.

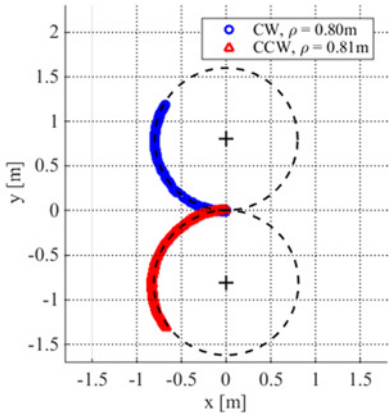

Fig. 7 Robot path recorded by the positioning sensor and the circular fit results

- Nominal wheelbase, $L_{nominal}$: 0.31 m
- Nominal tread, $b_{nominal}$: 0.30 m
- Nominal wheel diameter, $D_{R(L)\ nominal}$: 0.1005 m
- Encoder pulses per wheel revolution, Re: 1200

In preliminary experiments, steering angle calibration was carried out. To calibrate the steering angles for each control input, the actual paths of the robot were tracked. The actual pose of the robot was recorded using a Stargazer commercial absolute positioning sensor.[15]

Fig. 7 shows the recorded robot path and the circular fit results. For the given control input to the steering servo motor, the curvature of the robot path was almost constant. Circular fitting allows the radius of

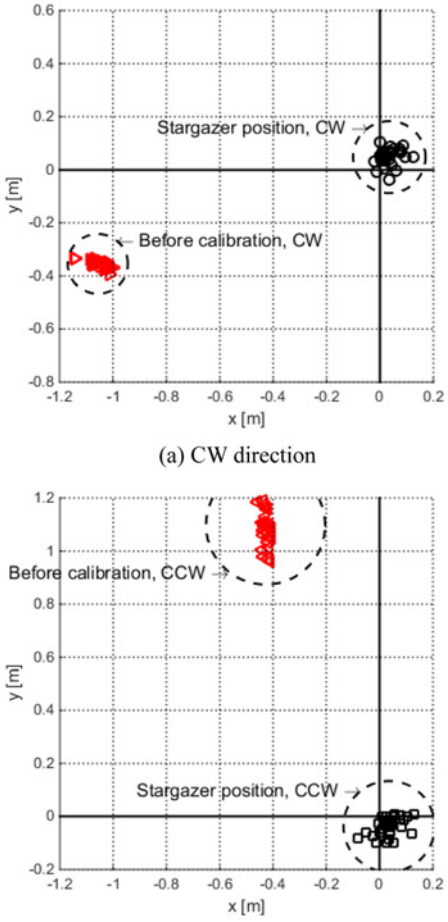

Fig. 8 Final position of the robot after the test runs

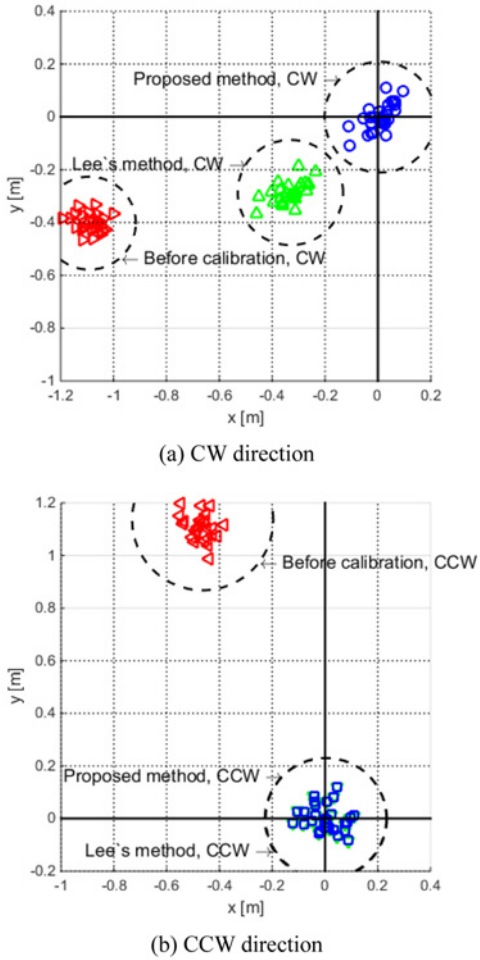

Fig. 9 Position errors after calibration. The estimated positions were compared with the measured by Stargazer positions

Table 1 Mean of the final pose after the test runs

		x (m)	y (m)	θ (°)
Stargazer pose	CW	0.03	0.05	3.0
	CCW	0.04	-0.04	-2.1
Before calibration	CW	-1.06	-0.35	-71.8
	CCW	-0.43	1.10	-51.3

Table 2 Resultant kinematic parameters

	E_b	E_d
Lee's method	0.9969	1.0298
Proposed method	1.0351	1.0426

curvature of the robot path to be computed. The steering angle for the given control input can then be calculated from the radius of curvature of the robot path.

After the preliminary experiments, odometry calibration was conducted. During the odometry calibration, the robot was driven along a pre-programmed test track with open-loop control. In order to consider the effect of nonsystematic errors, the test run was repeated 30 times in each direction.

Fig. 8 and Table 1 show the final pose after the test run. In Fig. 8 and Table 1, Stargazer pose means the pose recorded by the Stargazer sensor,[18] and Before calibration means the pose estimated from the encoder data before calibration. The robot was driven relatively accurately along the pre-programmed test track in spite of the open-loop control. However, the estimated robot poses were inaccurate because of systematic errors.

Table 2 presents the resultant kinematic parameter values after the calibration. The kinematic parameter values were estimated using Lee's method and the proposed method. The resultant kinematic parameter values were estimated by Lee's method and the proposed method were different. The resultant kinematic parameter values were E_b = 0.9969 and E_d = 1.0298 by using the Lee's methods. By using the proposed method, the resultant kinematic parameter values were E_b = 1.0351 and E_d = 1.0426.

Fig. 9 and Table 3 present the pose errors after calibration. Before calibration, the position RMSE(Root Mean Square Error) was 1.69 m. The orientation RMSE was 91.9°. After the calibration using Lee's method, the position RMSE was reduced to 0.39 m, and the orientation RMSE was reduced to 18.7°. After the calibration using the proposed method, the position RMSE was reduced to 0.12 m, and the orientation RMSE was reduced to 4.3°. The Odometry accuracy of the proposed method was about four times higher than that of the Lee's method. This result clearly shows the advantage of using the proposed method. The t-test results that comparing the mean difference between the Lee's

Table 3 Pose errors after calibration

		Position (m)	Orientation (°)
Before calibration	CW	1.16	-74.8
	CCW	1.23	-53.4
	RMSE	1.69	91.9
Lee's method	CW	0.39	-18.4
	CCW	0.08	3.3
	RMSE	0.39	18.7
Proposed method	CW	0.09	3.2
	CCW	0.08	2.9
	RMSE	0.12	4.3

Table 4 Results of t-tests for equality of means of the proposed method against that of Lee's method

Case		*t*-value	Degree of freedom	*p*
Position error	CW	15.986	29	0.000
	CCW	4.579	29	0.000
Orientation error	CW	-49.246	29	0.000
	CCW	26.458	29	0.000

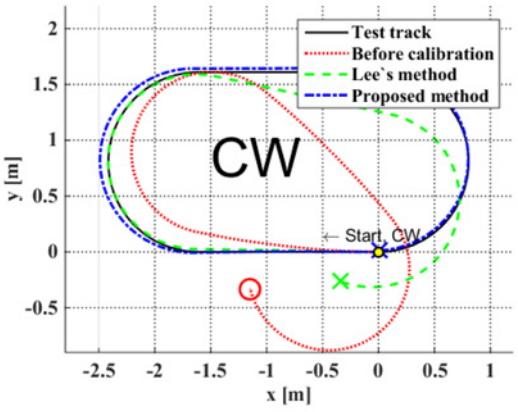

(a) CW direction

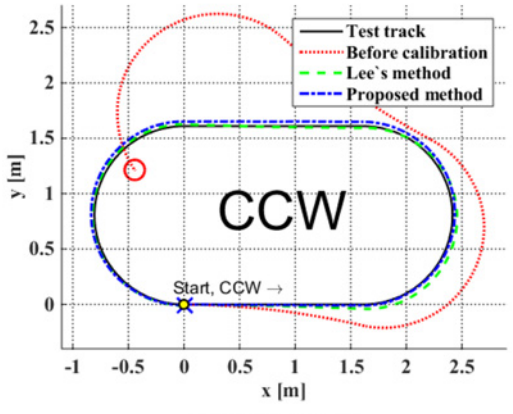

(b) CCW direction

Fig. 10 Robot path during the calibration experiments

method and the proposed method are presented in Table 4. As shown in the Table 4, the results between the compared methods have different mean value with a significance level $p<0.05$ (95% confidence level).[20]

Fig. 10 shows the estimated robot paths during the calibration experiments. It can be seen that not only the final position but also the estimated robot path approached the test track. From Fig. 10(a), it can be seen that the calibrated robot path of the proposed method was almost with the same as the test track. However, the calibrated robot path of the Lee's method was different. This means that errors caused by small-angle approximations can reduce the calibration accuracy. The experimental results verify that accurate odometry calibration is possible using the proposed method.

4. Conclusions

In this paper, a calibration method using experimental orientation errors is proposed. When the final position errors are used to calibrate odometry errors, small-angle approximations are required in the conventional method. This means that errors caused by small-angle approximations can reduce the calibration accuracy. Using experimental orientation errors instead of position errors, these approximation errors can be eliminated, and the calibration accuracy can be improved. Furthermore, the proposed scheme is advantageous because of the experimental convenience. The experimental measurement of orientation is much easier than the measurement of position. The orientations can be easily measured by onboard inertial sensors. However, environmental modifications are required for measurement of positions in most cases. For example, environmental modifications includes installation of artificial landmarks. The proposed calibration experiments can be easily carried out in both indoor and outdoor environments. The presented experimental results show that resultant performance of the proposed scheme is superior to the results of the previous research.

ACKNOWLEDGEMENT

This Research was supported by the NRF, MSIP (NRF-2014R1 A2A1A10049634), also supported by the Industrial Convergence Core Technology Development Program (No. 10063172) funded by MOTIE, also supported by Agriculture, Food and Rural Affairs Research Center Support Program (714002-07), MAFRA, also supported by the COMPA, MISP (2016K000138), Korea.

REFERENCES

1. Bashiri, M., Vatankhah, H., and Ghidary, S. S., "Hybrid adaptive Differential Evolution for Mobile Robot Localization," Intelligent Service Robotics, Vol. 5, No. 2, pp. 99-107, 2012.
2. Cheng, P.-Y. and Chen, P.-J., "Navigation of Mobile Robot by using D++ Algorithm," Intelligent Service Robotics, Vol. 5, No. 4, pp. 229-243, 2012.
3. Thrun, S., Burgard, W., and Fox, D., "Probabilistic Robotics," MIT Press, pp. 117-147, 2005.
4. Borenstein, J., Everett, H., and Feng, L., "Where am I? Sensors and Methods for Mobile Robot Positioning," www-personal.umich.edu/

~johannb/Papers/pos96rep.pdf (Accessed 5 JUL 2016)

5. Borenstein, J. and Feng, L., "Measurement and Correction of Systematic Odometry Errors in Mobile Robots," IEEE Transactions on Robotics and Automation, Vol. 12, No. 6, pp. 869-880, 1996.
6. Siegwart, R., Nourbakhsh, I. R., and Scaramuzza, D., "Introduction to Autonomous Mobile Robots," MIT Press, pp. 265-367, 2011.
7. Borenstein, J. and Feng, L., "Gyrodometry: A New Method for Combining Data From Gyros and Odometry in Mobile Robots," Proc. of IEEE International Conference on Robotics and Automation, Vol. 1, pp. 423-428, 1996.
8. Komoriya, K. and Oyama, E., "Position Estimation of a Mobile Robot using Optical Fiber Gyroscope (OFG)," Proc. of IEEE/RSJ/GI International Conference on Intelligent Robots and Systems, Vol. 1, pp. 143-149, 1994.
9. Lee, K., Jung, C., and Chung, W., "Accurate Calibration of Kinematic Parameters for Two Wheel Differential Mobile Robots," Journal of Mechanical Science and Technology, Vol. 25, No. 6, pp. 1603-1611, 2011.
10. Jung, C. and Chung, W., "Calibration of Kinematic Parameters for Two Wheel Differential Mobile Robots by using Experimental Heading Errors," International Journal of Advanced Robotic Systems, Vol. 8, No. 5, pp. 134-142, 2011.
11. Jung, C. and Chung, W., "Accurate Calibration of Two Wheel Differential Mobile Robots by using Experimental Heading Errors," Proc. of IEEE International Conference on Robotics and Automation (ICRA), pp. 4533-4538, 2012.
12. McKerrow, P. J. and Ratner, D., "Calibrating a 4-Wheel Mobile Robot," Proc. of IEEE/RSJ International Conference on Intelligent Robots and Systems, Vol. 1, pp. 859-864, 2002.
13. Lee, K. and Chung, W., "Calibration of Kinematic Parameters of a Car-Like Mobile Robot to Improve Odometry Accuracy," Proc. of IEEE International Conference on Robotics and Automation, pp. 2546-2551, 2008.
14. Lee, K., Chung, W., and Yoo, K., "Kinematic Parameter Calibration of a Car-Like Mobile Robot to Improve Odometry Accuracy," Mechatronics, Vol. 20, No. 5, pp. 582-595, 2010.
15. Atmel Co., Ltd., "ATmega128," http://www.atmel.com/devices/ATMEGA128.aspx (Accessed 14 JUL 2016)
16. NewTC Co., Ltd., "AVR MEGA 128 PRO Development Kit," http://www.newtc.co.kr/dpshop/shop/item.php?it_id=1458730878 (Accessed 14 JUL 2016)
17. Nidec Copal Electronics Corp., "Rotary Encoder RE12D," http://www.nidec-copal-electronics.com/e/product/files/file/bbacb8cc4ab651a54cba60a4d60eafd9f8ba2b1d.pdf (Accessed 18 JUL 2016)
18. Hagisonic Co., Ltd., "tarGazer_Guide," http://eng.hagisonic.kr/downLoad.html?cate=community&uid=338&fileName=129231125 2928980&downName=StarGazer_Guide_02.0904.16(English).pdf (Accessed 14 JUL 2016)
19. Firmtech Co., Ltd., "Bluetooth Serial Adapter FB100AS User Guide," http://www.firmtech.co.kr/default/img/eng/manual/fb100as/FB100AS_User_Guide(Eng).pdf (Accessed 14 JUL 2016)
20. Peck, R., Olsen, C., and Devore, J. L., "Introduction to Statistics and Data Analysis," Cengage Learning, 4th Ed., pp. 638-658, 2015.